

OBSERVATIONS OF THE MARTIAN CLIMATOLOGY.

D. M. Kass, A. Kleinböhl, D. J. McCleese, J. T. Schofield, *Jet Propulsion Laboratory/California Institute of Technology, Pasadena, California, USA (David.M.Kass@jpl.nasa.gov), M. D. Smith,* *NASA Goddard Space Flight Center, Greenbelt, Maryland, USA.*

Introduction:

The martian atmosphere exhibits significant interannual variability at some seasons. And yet, at other seasons it is impressively repeatable.

During the southern summer (perihelion) or dusty season most years are very different due to the extent and location of the dust activity [e.g. Zurek and Martin, 1993]. Not surprisingly, the atmospheric temperature and structure respond very differently to the different Mars years. In other seasons, especially during northern summer, the atmosphere is remarkably similar from year to year [Cantor *et al.*, 2002]. The lack of interannual variability comes despite the large variations in the dusty season.

By combining MCS (on MRO), TES (on MGS) and THEMIS (on Odyssey) observations we have constructed an atmospheric climatology spanning over 6 Mars years (MY 24 through MY 30). We are currently examining the temperature structure of the lower atmosphere (~ 50 Pa or 25 km) and examining the interannual variability at various seasons. In addition, the MCS observations cover over 2 Mars years and allow the structure of the middle atmosphere to be examined.

Datasets:

We have taken the temperature retrievals from each of the instruments and binned them into latitude/Ls bins. We are looking at the 50 Pa surface (or ~ 25 km), and for MCS we are also looking at 5 Pa (~ 45 km) and 0.5 Pa (~ 65 km).

While all three instruments are measuring atmospheric temperature they are using different techniques and are on different platforms. This results in a number of subtle differences that need to be taken into account when considering the data. The binning was selected independently for each dataset. It was optimized to be as fine as possible while matching each dataset's intrinsic properties.

Mars Climate Sounder. MCS is an infra-red 9 channel limb staring radiometer [McCleese *et al.*, 2007]. The retrieval algorithm [Kleinböhl *et al.*, 2009] produces vertical profiles of temperature, dust and water ice extinction versus pressure. The MCS detectors have a 5 km vertical resolution on the limb, providing a half scale height resolution. The retrieved profiles generally extend from the surface to ~ 80 km.

The retrievals were binned in 5° latitude by 2° Ls bins. MCS is on the MRO orbiter in a near polar sun-synchronous orbit with a local mean solar time of 3 AM/3 PM at the equator [Zurek and Smrekar, 2007]. The MCS observations start at Ls = 110° in

MY 28 and continue to the present.

Thermal Emission Spectrometer. TES is primarily a nadir sounding infra-red spectrometer with 6 cm^{-1} or 12 cm^{-1} resolution [Christensen *et al.*, 2001]. The retrieval algorithm produces vertical profiles of temperature and column integrated dust and water ice and water vapor opacities [Conrath *et al.*, 2000 and Smith, 2004]. For this work we have only used the nadir geometry TES observations. The spectral resolution in the nadir geometry provide a one scale height vertical resolution and coverage from the surface to ~ 40 km.

The TES retrievals were binned into 2° latitude by 2° Ls bins. TES is on the MGS orbiter in a near polar sun-synchronous orbit with a local mean solar time of 2 AM/2 PM at the equator. The TES observations start at the beginning of the analysis (Ls = 102° in MY 24). They continue through to Ls = 82° in MY 27.

Thermal Emission Imaging System. THEMIS is a visible and infra-red camera [Christensen *et al.*, 2003]. Some of its wavelengths provide atmospheric information and retrievals of temperature, dust column opacity and water ice column opacity [Smith, 2009]. Unlike MCS or TES, THEMIS is not a global mapping instrument and it only takes occasional images. It does have a regular (coarse resolution) grid sequence it performs for atmospheric monitoring. Each image is then averaged to produce mean atmospheric conditions.

THEMIS has a $15\text{ }\mu\text{m}$ band used for temperature retrievals. This provides the atmospheric temperature centered at ~ 50 Pa (25 km) with a ~ 2 scale height vertical weighting function (~ 20 km) [Smith, 2009].

The THEMIS temperatures were binned into 5° latitude by 5° Ls bins. THEMIS is on the Odyssey orbiter in a near polar sun-synchronous orbit with a local mean solar time varying between 3 PM/3 AM and 6 PM/6 AM at the equator. The THEMIS observations start at Ls = 330° in MY 25 and extend through to the present. To avoid confusion, we only use the THEMIS data after the end of the TES data and before the start of the MCS data (Ls = 82° in MY 27 through Ls 110° in MY 28). The regions of overlap are useful for validation of the instruments.

Preliminary Analysis:

Figure 1 shows the zonal mean atmospheric temperatures at 50 Pa from the three instruments, covering over 6 Mars Years.

Figure 1. Daytime and Nighttime zonal mean binned temperatures at 50 Pa (~ 25 km) from TES, THEMIS and MCS.

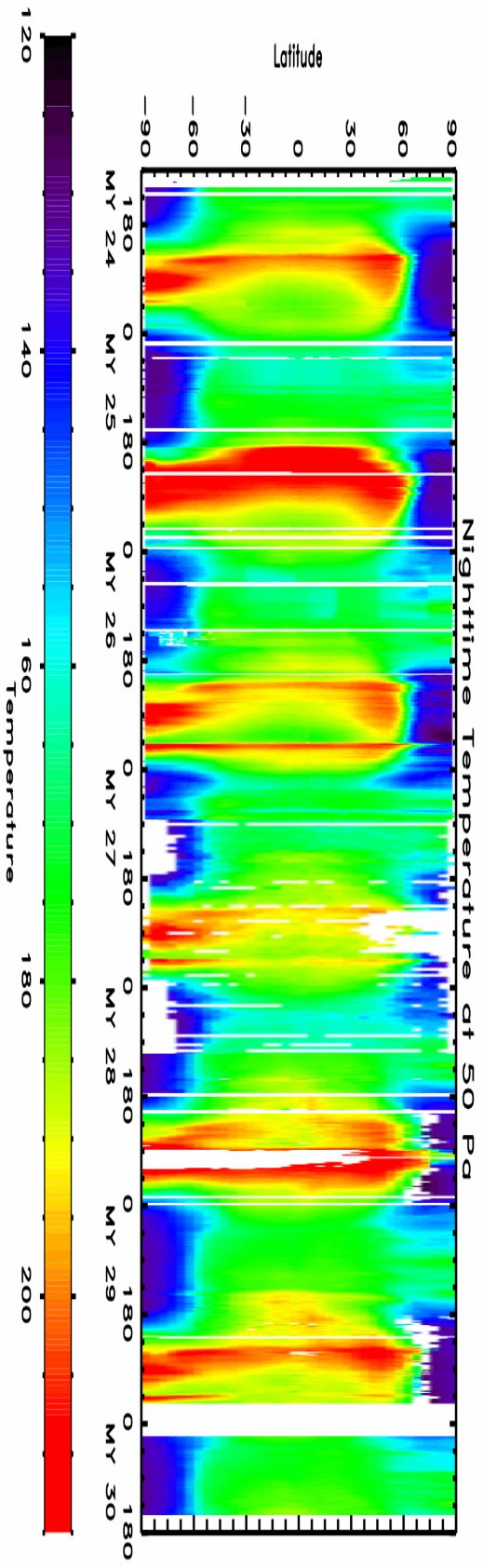
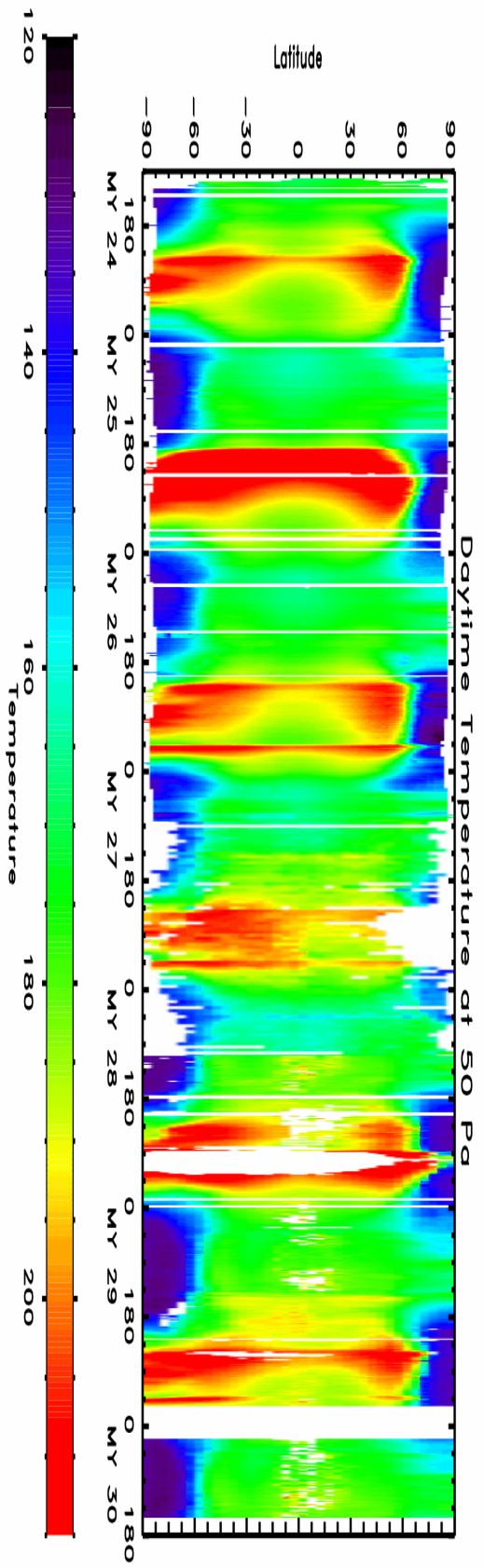


Figure 2. Same daytime temperature data as shown in figure 1. A different temperature scale has been used to emphasize the atmospheric warming due to the dust.

Several basic aspects of the martian atmosphere are evident. The first is the very large temperature contrast between the dusty southern summer and the cooler (icy) northern summer. The temperature differences are apparent in both hemispheres. Also apparent are the cold regions due to the winter polar vortex that form over the winter pole.

Major Dust Events. The majority of the elevated temperatures seen in the temperature field are directly or indirectly associated with dust storms, especially those that loft dust out of the boundary layer. Figure 2 shows a different temperature stretch to emphasize the warmest temperatures, mostly driven by the dust. The corresponding nighttime temperature structure (not shown) is very similar.

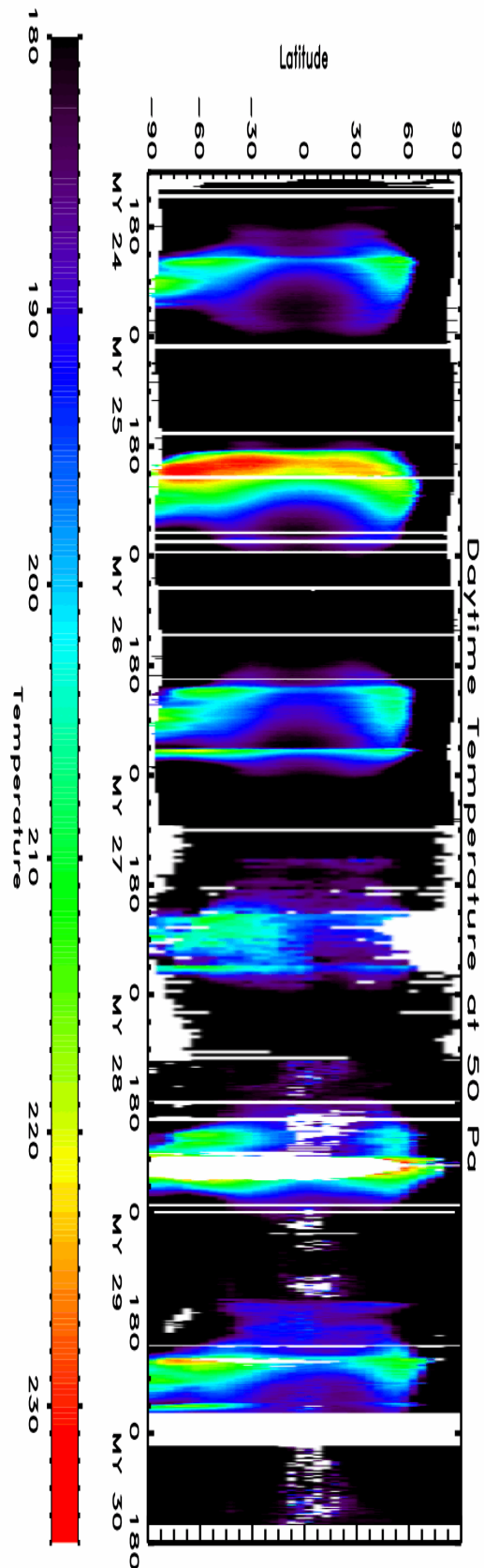
In the 6 Mars Years covered by the climatology, there are two years with global dust storms, MY 25 and MY 28. These two storms are very different. The one in MY 25 is the earliest global storm on record, starting around the equinox. While MY 28 has a very late, solstice storm (similar to the season of the Viking 1977b storm). Unfortunately, MCS is unable to retrieve the temperature at the height of the MY 28 storm due to the opacity along the limb path.

One of the significant differences between the two storms is that the early one does not penetrate or disrupt the northern polar vortex while the warming from the solstice storm reaches all the way to the pole. This results in the northern polar region showing the largest overall temperature increase of around 100 K (from ~ 130 K to ~ 230 K).

The other four years have large storms where the dust mostly remains confined to the southern hemisphere. All of these storms trigger significant warming in the northern hemisphere despite little increase in the dust. This warming is presumably due to the dynamical (adiabatic) warming from modifying the Hadley circulation although there may also be a contribution from changes to the global thermal tide.

In the southern hemisphere, these storms appear to have two phases (the data in MY 27 is marginal, however it seems to show some of the same features). The first shows warming in the southern mid-latitudes (~ 45 S to ~ 60 S). This is accompanied by an almost instantaneous response at ~ 45 N. This is followed by an event that starts essentially at the south pole and spreads to ~ 60 S at $L_s = 270^\circ$ while lasting for almost half a season (45° of L_s). The initial phase is warmer in MY 29 and the daytime temperature signatures of the two have somewhat merged together (a finer examination shows that they are distinct [Kass *et al.*, 2010]).

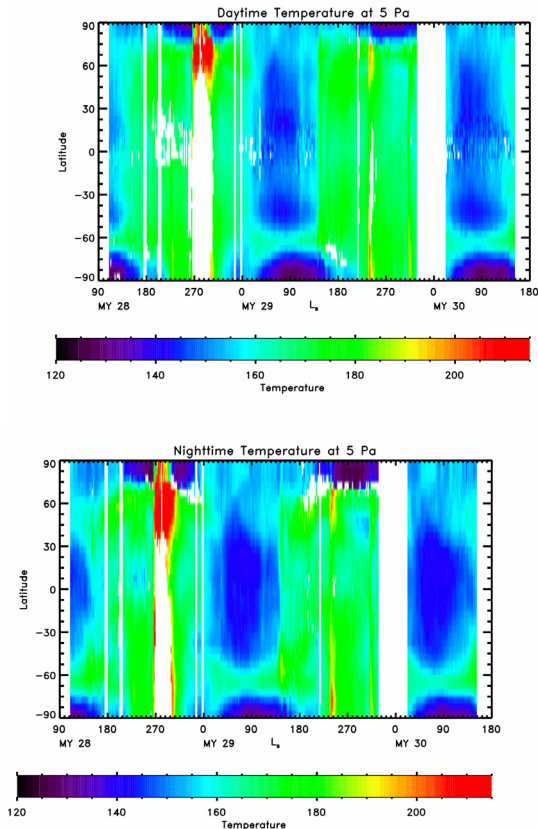
All four years without a global events also have a small event right around $L_s = 315^\circ$, well after the larger storm has essentially died away (this is best



seen in Figure 1). The peak temperature impact from this storm is seen at very high southern latitudes with warming at most latitudes in some years. In MY 28, the global storm is still ongoing at that season, however MY 25 seems to be an exception.

Middle Atmosphere: MCS retrievals cover the middle martian atmosphere (~40 km to ~80 km), allowing the examination of the climatology at 5 Pa (~45 km) and 0.5 Pa (~65 km). Figures 3 and 4 show the temperature structure at these pressures.

Figure 3. Daytime and Nighttime zonal mean temperatures at 5 Pa (~45 km) from MCS.



The strong warming above the northern polar vortex during the MY 28 dust storm is very evident even in the middle atmosphere. The warming extends all the way 65 km (and is still just distinguishable at the top of the MCS coverage ~80 km). The initial pulse of the regional dust activity in MY 29 also produced noticeable warming at 5Pa, but there is no significant signal at 0.5 Pa.

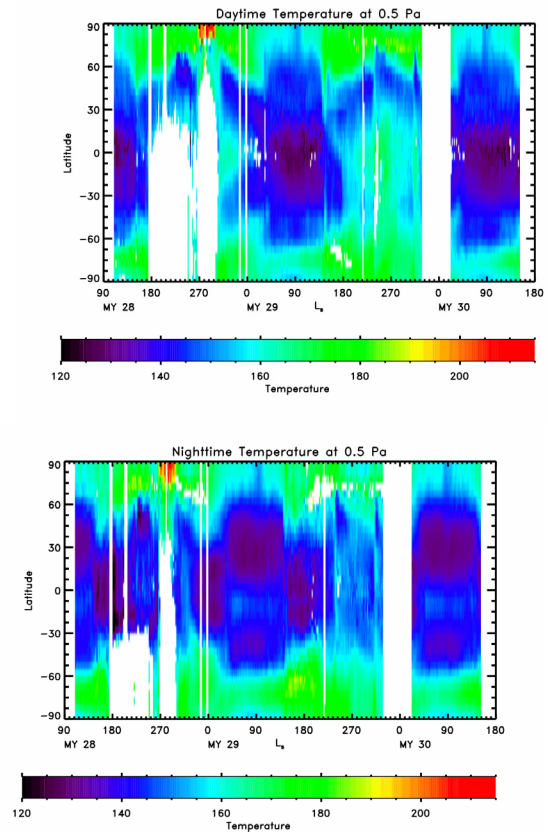
In the southern winter, there is a strong warming seen in the southern polar regions. However this is persistent throughout the season. The warming extends to the pole at 0.5 Pa. However, at 5 Pa, the peak is at ~70 S and there is a small very cold region poleward of the warming.

Middle Atmosphere Diurnal Tide Signature. At 0.5 Pa, a very noticeable complex, seasonally varying, pattern exists in the temperature structure. This is due to the diurnal thermal tide [Lee *et al.*, 2009].

In the daytime, a pair of cold anti-nodes exist at

~50° latitude (both north and south) after the disruption from the MY 28 dust storm ($L_s \sim 305^\circ$). They converge on the equator by $L_s \sim 30^\circ$ and intensify in the process. After remaining with a very cold equatorial region through $L_s \sim 145^\circ$, a pair of branches move poleward.

Figure 4. Daytime and Nighttime zonal mean temperatures at 0.5 Pa (~65 km) from MCS.



The nighttime response is different with a “box” pattern of very cold anti-nodes. They are centered at the equator during the early season. They abruptly move to the mid-latitudes when the daytime feature develops at the equator. The pattern again reverses itself when the daytime anti-nodes start moving poleward again.

References: Cantor *et al.* (2002), *JGR* 107, doi: 10.1029/2001JE001588; Christensen *et al.* (2001), *JGR* 106, 23823-23871; Christensen *et al.* (2003), *Space Sci. Rev.* 110, 85-130; Conrath *et al.*, (2000), *JGR* 105, 9509-9520; Kass *et al.* (2010), *Mars Dust Cycle Workshop*, NASA/CP-2010-216377, 15; Kleinböhl *et al.* (2009), *JGR* 114, E10006, doi: 10.1029/2009JE003358; Lee *et al.* (2009), *JGR* 114, E03005, doi: 10.1029/2008JE003285; McCreese *et al.* (2007), *JGR*, 112, E05S06 doi: 10.1029/2006JE002790; Smith (2004), *Icarus* 167, 148-165; Smith (2009), *Icarus* 202, 444-452; Zurek and Martin (1993), *JGR* 98, 2347-2399; Zurek and Smrekar (2007), *JGR*, 112, E05S01, doi: 10.1029/2006JE002701.

Acknowledgement: This work was carried out at the Jet Propulsion Laboratory, California Institute of Technology under a contract with the National Aeronautics and Space Administration.